NSLS II TECHNICAL NOTE BROOKHAVEN NATIONAL LABORATORY	NUMBER **210**
AUTHORS: **K. Attenkofer**	DATE: **3/21/2016**
ISS Mirror Mis-steer Analysis	

1 Introduction

This technical note discusses a specific case of mirror mis-steering at the ISS beamline at sector 8-ID. The heat load and potential damage to the secondary bremsstrahlung shield mounted to the mask MA2 will be discussed for the worst case of mis-steering of the mirror CM1 as shown in the ray trace drawing PS-ISS-RAYT-0001, page 4. This note is a response to the first recommendation of the Radiation Safety Committee Report. A model of the mask-secondary bremsstrahlung shield is shown in **Error! Reference source not found.**.

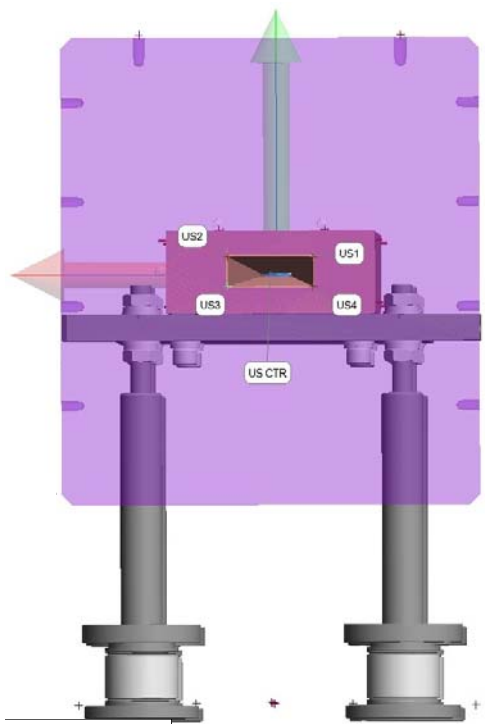

Figure 1: Mask 2 with the W Secondary Bremsstrahlung Shield

2 The Beamline Configuration

For the following calculations it is assumed that both DW100 wigglers of 8-ID are fully closed, the front end slits wide open, and all filters of the filter box removed or otherwise specifically described. CM1, the first mirror, is reflecting the beam with an incident angle of 8 mrad, using the Pt-coated area of the mirror.

2.1 Heat Load Configuration

The Source

The spectrum used in the following discussion is a DW100 spectrum with 70 periods, 500 mA beam current and an acceptance of 1.1 mrad x 0.1 mrad. These numbers are consistent with Table **1**.

Table 1: Source File for Power Calculation

TITLE	'DW100'	NEE	10000
ENERGY	3.00000	D	30.0000
CUR	500.000	XPC	0.00000
PERIOD	10.0000	YPC	0.00000
N	70.0000	XPS	33.0000
KX	0.00000	YPS	3.00000
KY	16.8180	NXP	50
EMIN	1000.00	NYP	50
EMAX	250000.		

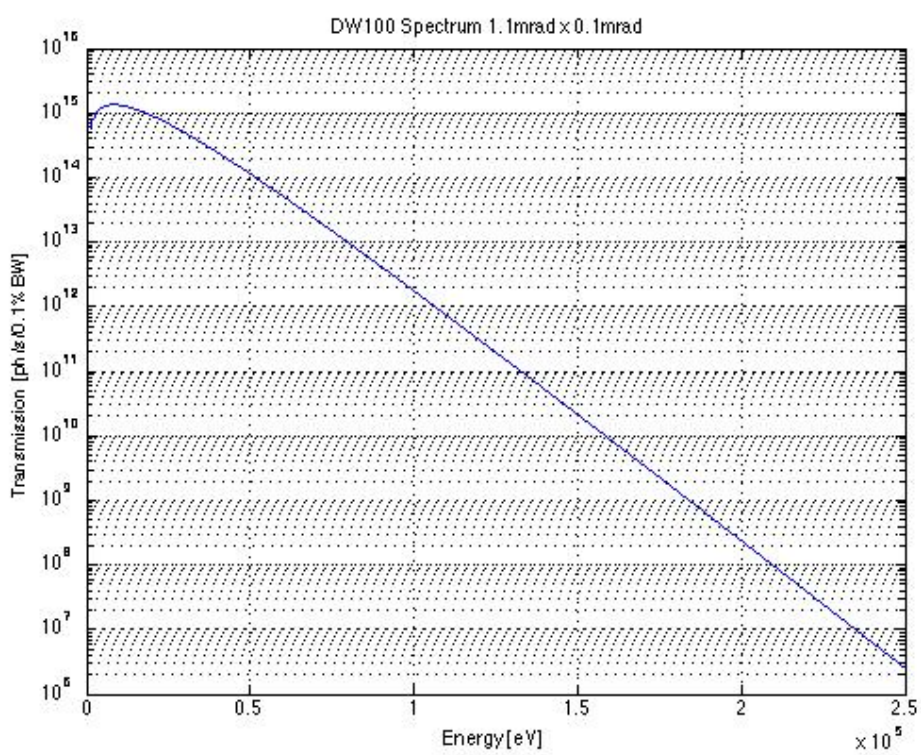

Figure 2: Calculated Spectrum in Units of Photons/s/0.1%BW using ws (xop) using the Parameter File Shown in Table 1

The reflected beam

Mask MA1, the defining mask for CM1, has a 1.0x0.1 mrad^2 acceptance, reducing the total power by 0.91. Taking the reflectivity of a Pt-coated mirror with an incident angle of 8 mrad into account, the total power of the reflected beam which can hit mask MA2 is **1.25k W**. The spectral distribution of the reflected beam is shown in Figure 3.

In the case where the appropriate pyrolytic graphite filter (80 layers of 70 μm thick Panasonic graphite) is used, the reflected power drops down to 86 W. The power spectrum for this case is shown in Figure 4.

An important, special case is if the beam hits the W-plate at the area that is not backed by the Cu mask; this corresponds to an incident beam angle at the mirror CM1 of 18 mrad or larger. The total reflected power of the x-ray beam is less than 275 W and less than 1 W, in a configuration which uses the graphite filters described above.

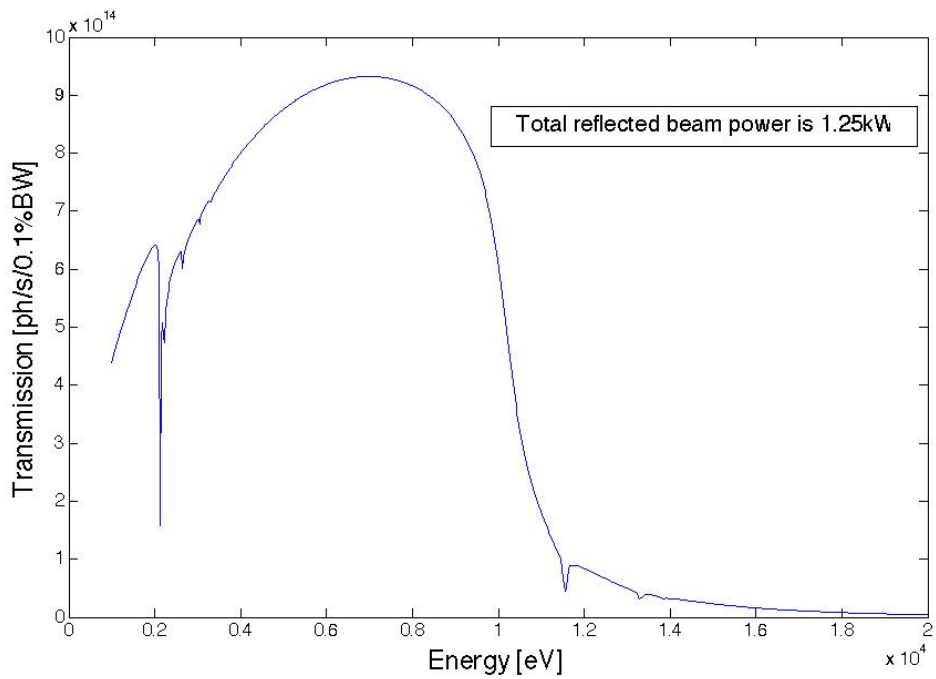

Figure 3: Flux of the reflected beam from a Pt-coated mirror (0.3 nm roughness) at 8 mrad incident angle. The cut-off energy is about 10 keV. The total reflected power is 1.25 kW.

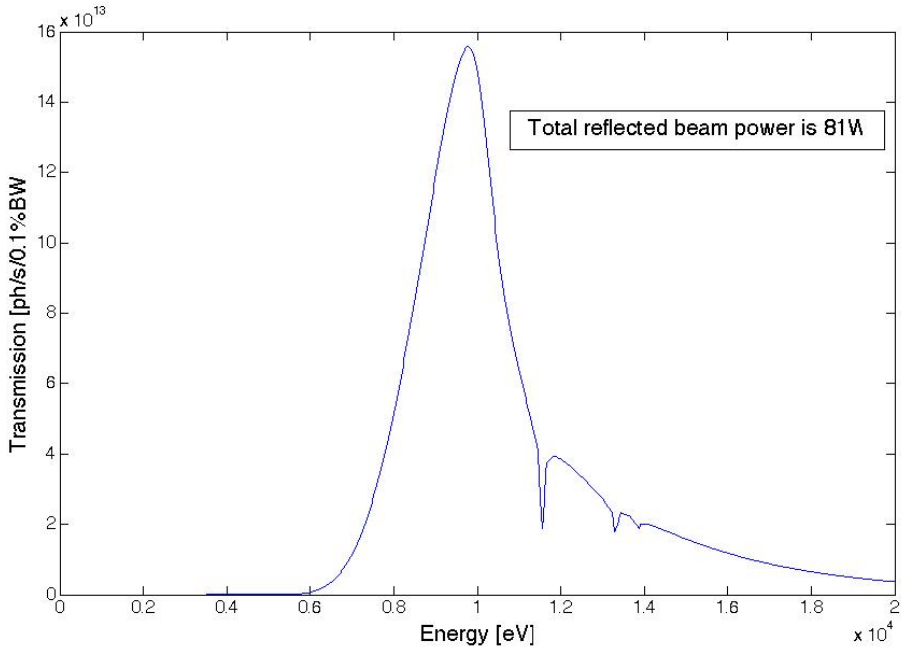

Figure 4: Identical configuration like in Figure 3 including the graphite filter for the high energy range of the beamline (80 layers of 70 mm thick Panasonic graphite). The total reflected power drops to 81W.

3 Thermal Behavior of Tungsten

The FEA analysis (see appendix A) of a similar case is shown in Figure 6; this analysis discusses the thermal behavior of a W-plate, hit by a 1.5k W x-ray beam (dimension 29.91 mm x 2.85 mm). Similar to the mask MA2, the W-plate is well connected to a cooled Cu-surface (see Figure 5). Radiation cooling is neglected. The calculation shows the thermal development of the various components for an exposure of the W-plate for 10 seconds. The system does not reach the equilibrium temperature, but the curve in Figure 6 can be easily extrapolated, showing that the maximal temperature is below 1500^0C and therefore below the melting temperature.

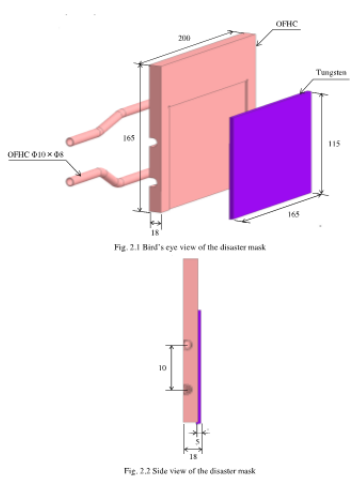

Figure 5: FEA Model of a Cooled W-Plate Exposed for 10s to a 1.5kW X-Ray Beam

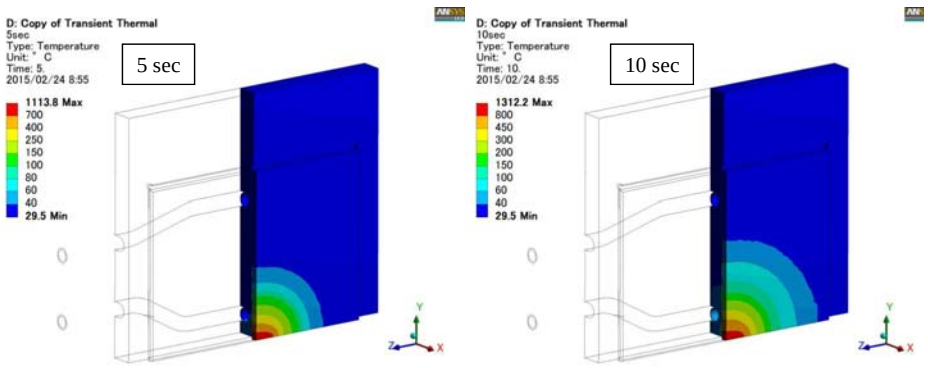

Temperature profile

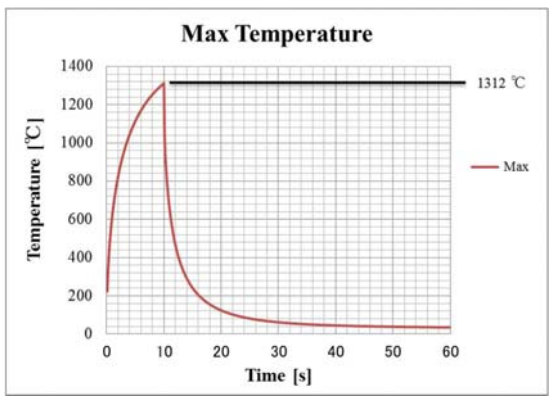

Time dependence of the maximum temperature

Figure 6: Transient thermal analysis of an indirect cooled W-plate hit for 10s by a 1.5k W x-ray beam. The equilibrium temperature is not reached after 10s but the asymptotic behavior of the graph indicates that the final temperature is close to 1400^0C to 1450^0C.

4 Conclusion

Three conclusions can be drawn:

1.) The exposure of the secondary bremsstrahlung shield to a 1.25 kW beam will not destroy the W shield, or any other radiation shielding component.

2.) A mis-steered beam with appropriate (as intentioned) graphite filters in place will expose the shield to a maximum power, which is far below 100 W.

3.) The reflected power of a beam which can hit the W-plate at a position which is not backed by the cooled Cu-masked, will be below 275 W. The thermal conductivity of the W-allow (about a third of Cu thermal conductivity) will be sufficient to remove this heat without damaging the shield. The heat load on the W-plate is negligible (<1W) if graphite filters are used.

One can conclude that under no operational conditions can the secondary bremsstrahlung shield be destroyed.

Appendix A

NSLS 2 ISS
Transient thermal analysis

- Synchrotron light irradiate the M2 Disaster Mask for 10 seconds -

Created by : Tsubota

1. Scope

We have performed the transient thermal analysis of the disaster mask at the NSLS-2 ISS beamline to evaluate the temperature profile. We assumed that the beam size at the disaster mask is H × V = 29.91 mm × 2.85 mm and absorbed power is 1500 W. And we assumed that the synchrotron light irradiate the disaster mask for 10 seconds. We made a calculation up to 50 seconds after irradiation. The analysis was done with using the FEA software ANSYS 14.0 Professional NLT.

The calculation results summary are listed in Table 1. The analysis results show that the disaster mask will not be melted within 10 second.

Table 2 shows the list of each figures.

	Results		Unit
	@ 10sec	@ 60sec※	
Maximum Temperature	1312	34.9	℃
Substrate Maximum Temperature	64.1	32.2	℃
Cooling pipe Maximum Temperature	57.6	31.7	℃
Substrate material : OFHC			

※ It indicates the time from the start of irradiation.

Table 1. Summary

Figure 2	Dimensional drawing	Page 2
Figure 3	Power input position	Page 3
Figure 4	Boundary conditions	Page 4
Figure 5	Calculation results	Page 5-11

Table 2. List of each figures

2. Dimensional drawing

Fig. 2.1and Fig. 2.2 show the dimensional drawing of the disaster mask. The concept of the design is that the tungsten endures the heat load for 10 second at first. And the cooling pipe gradually cool the model after irradiation. This can prevent the temperature of the cooling pipe becoming too large.

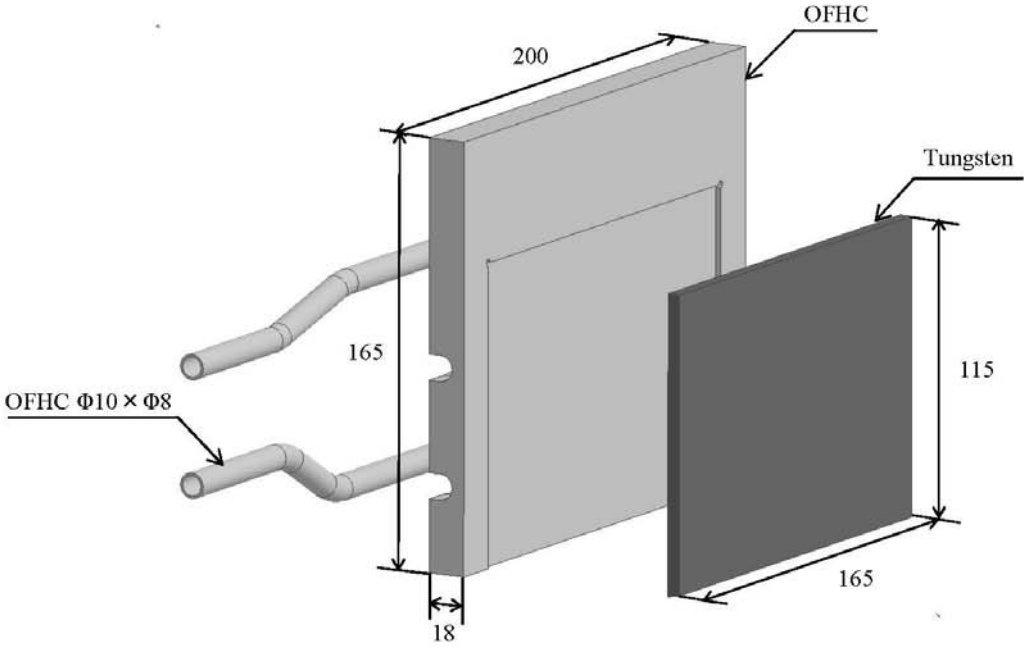

Fig. 2.1 Bird's eye view of the disaster mask

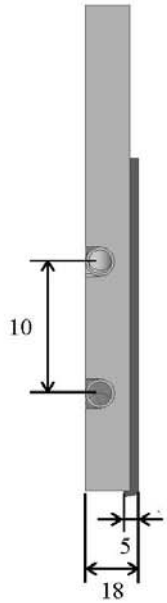

Fig. 2.2 Side view of the disaster mask

3. Power input position and physical properties of materials

The green area in Fig. 3.1 shows the heat input position at disaster mask. The disaster mask is set at 29.3 m and we assumed the maximum photon beam size is Horizontal × Vertical = 29.91 mm × 2.85 mm. The calculated total power absorbed in the disaster mask is 1500 W.
The Table 3.1 and Table 3.2 show the physical properties of materials used for calculation.

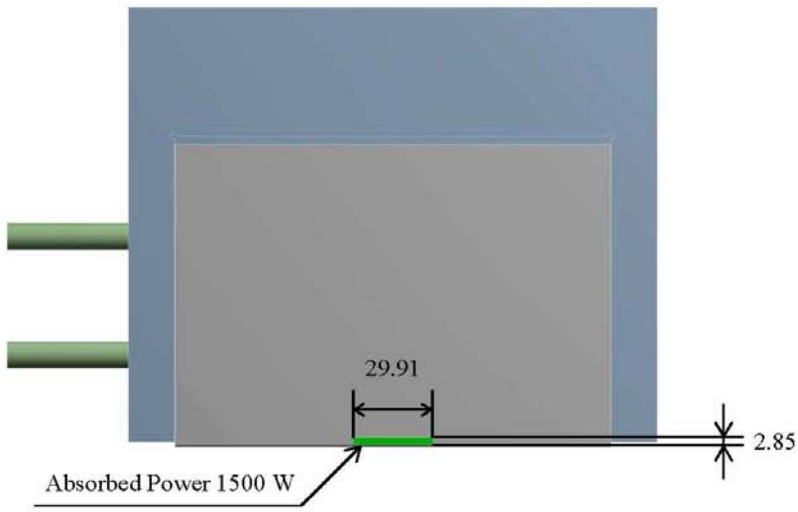

Fig. 3.1 Heat input position of disaster mask

		OFHC	Tungsten
Density	kg/m^3	8900	19250
Thermal Conductivity (300K)	W/m・K	Table 3.2	Table 3.2
Specific heat (300 K)	J/kg・K	380	138

Table 3.1 Physical properties of materials

4. Boundary conditions

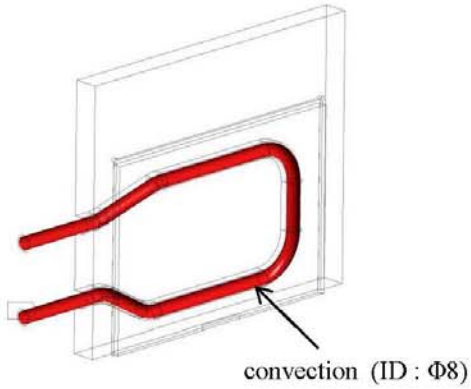

Fig. 4 Convection Surface

The calculation conditions

- Plate temperature before heating : 29.5 ℃
- Absorbed power : 1500 W (uniformed heat flux)
- Distance from the source : 30.9 m
- Beam size at disaster mask Position : Horizontal × Vertical = 29.91 mm × 2.85 mm
- OFHC – Tungsten thermal contact conductance : 1000 W/mm²·K
- Convection coefficient : 5500 W/m²·K (Flow rate : 3.1 l/min, Flow velocity : 1.0 m/s)
- Thermal radiation is not included

Temperature	Tungsten	OFHC
℃	W/m·℃	W/m·℃
26.85	178	398
76.85	170	394
126.85	162	392
326.85	139	383
526.85	128	371
726.85	121	357
926.85	115	342
1082.85		330
1126.85	111	
1526.85	103	
1926.85	97.7	
2326.85	93.8	
2726.85	91.3	

Table 3.2 Temperature dependence of Thermal Conductivity

5. Calculation results

5.1 Temperature profile (1-60 sec)

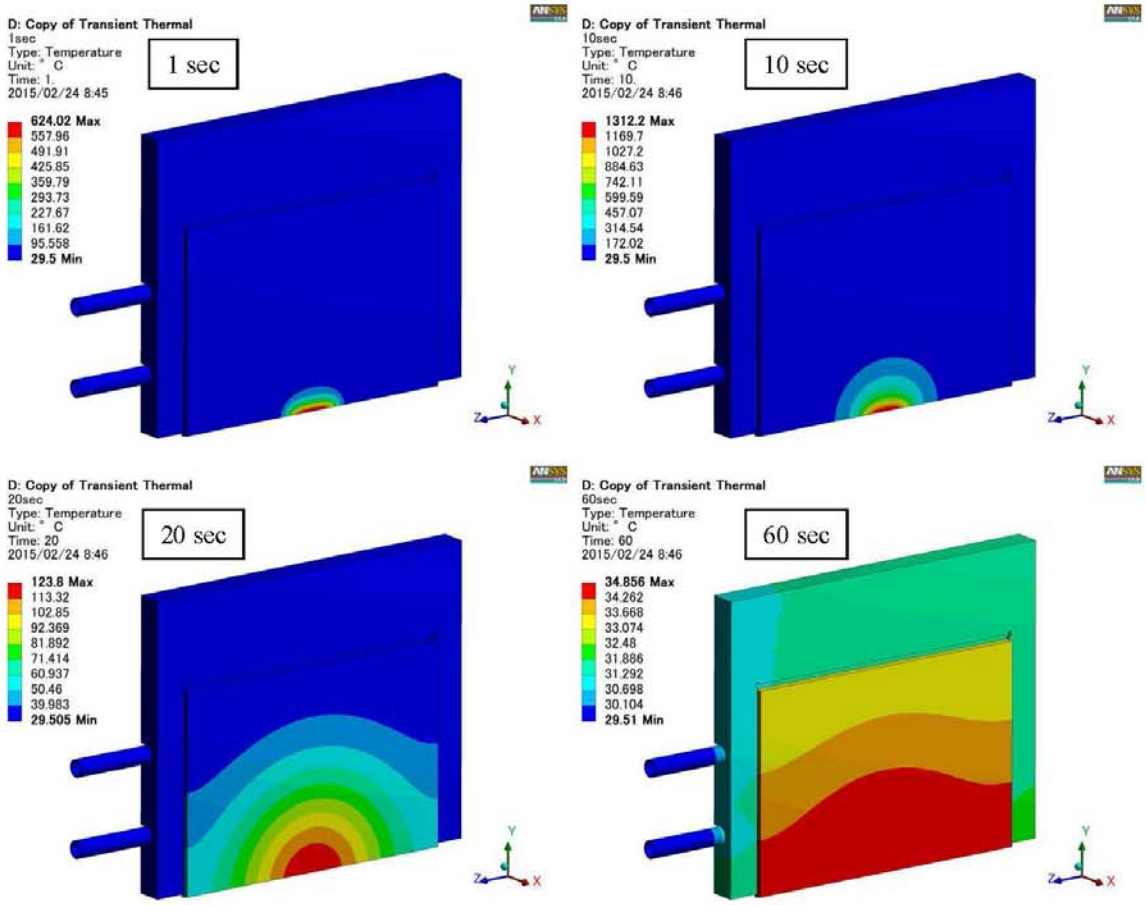

Fig. 5.1.1 Temperature profile

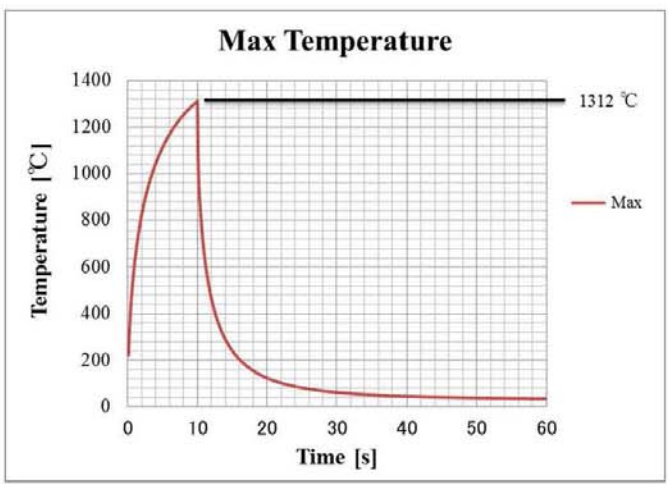

Fig. 5.1.2 Time dependence of the maximum temperature

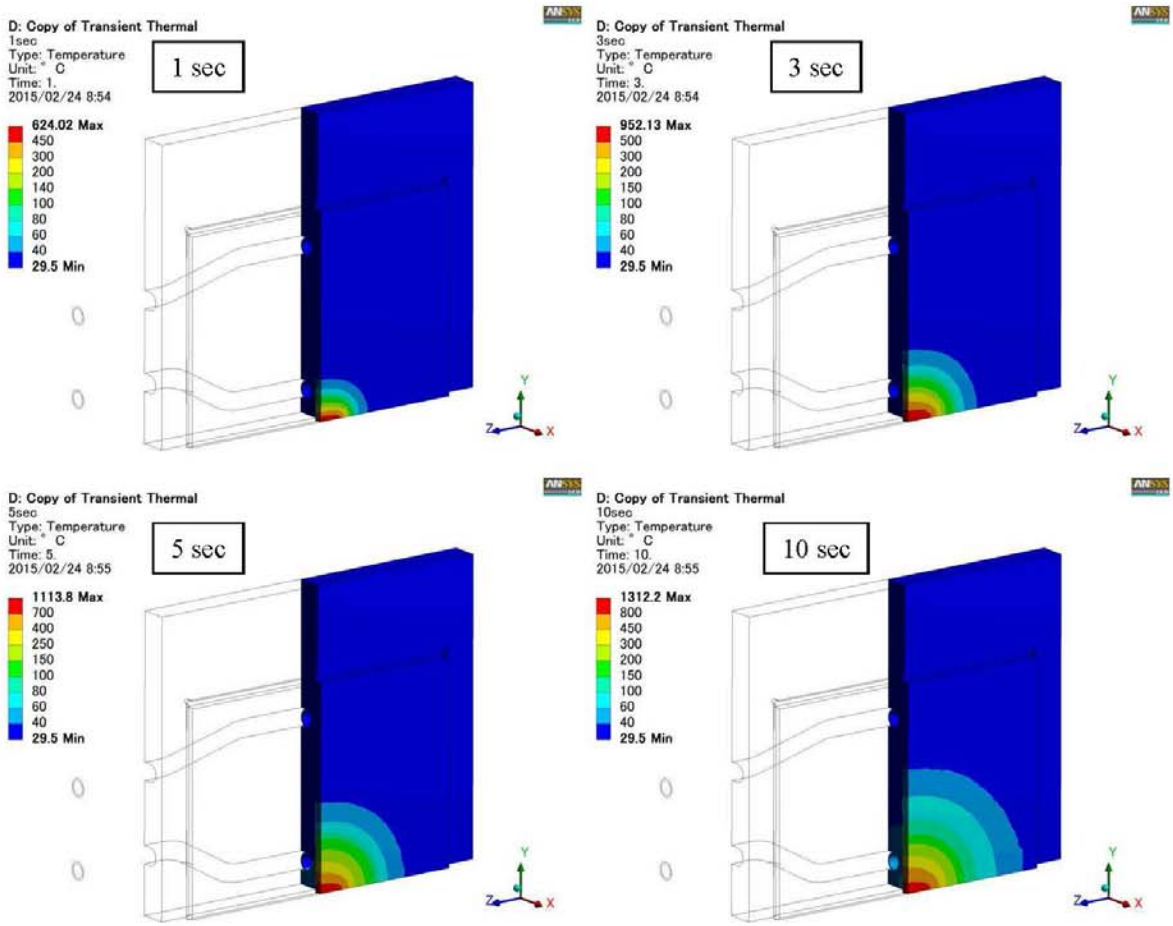

Fig. 5.1.3 Temperature profile

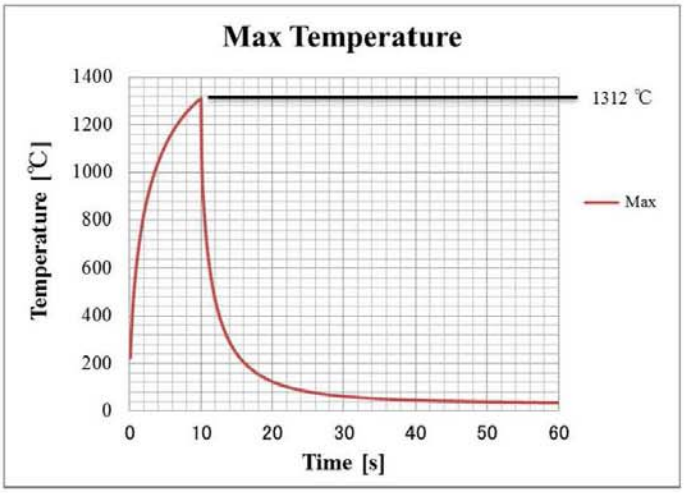

Fig. 5.1.4 Time dependence of the maximum temperature

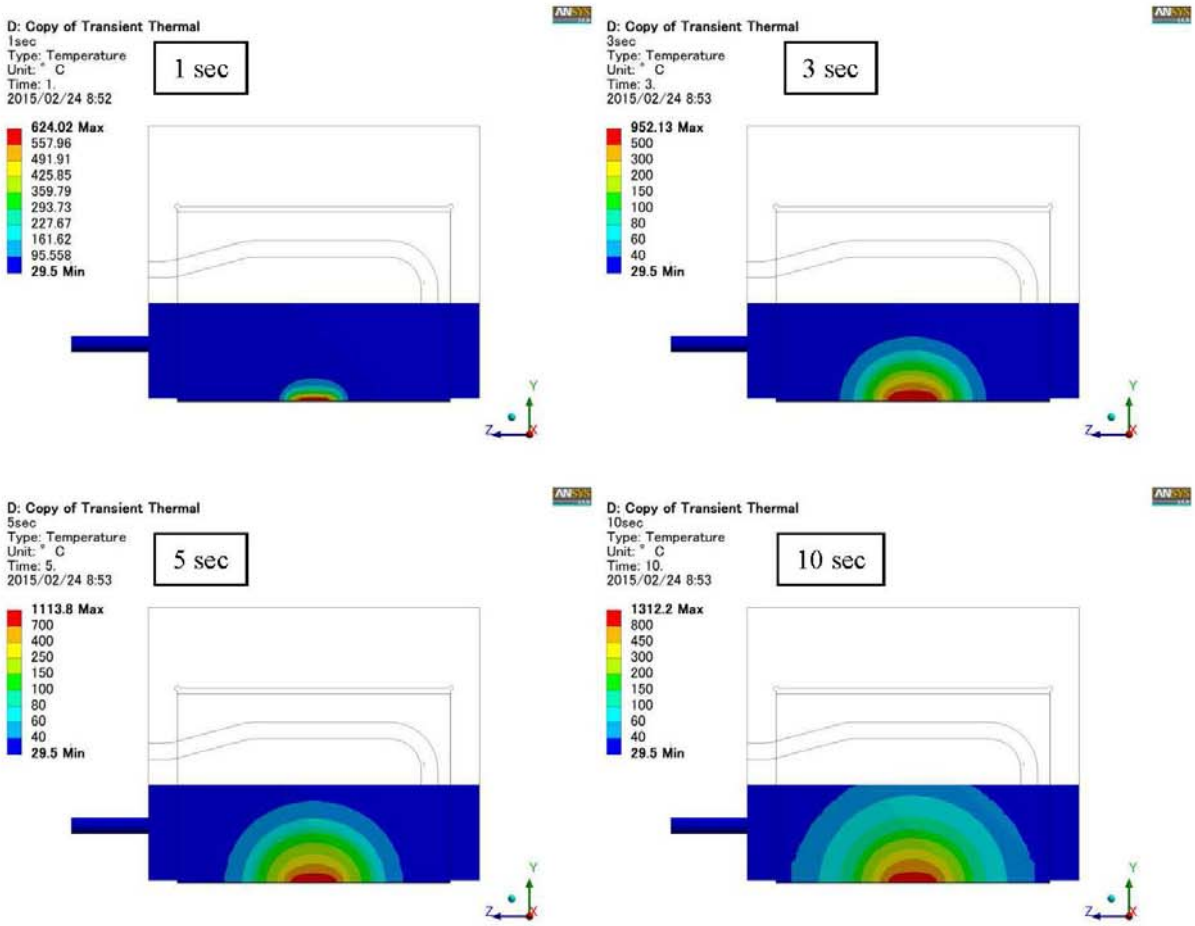

Fig. 5.1.5 Temperature profile

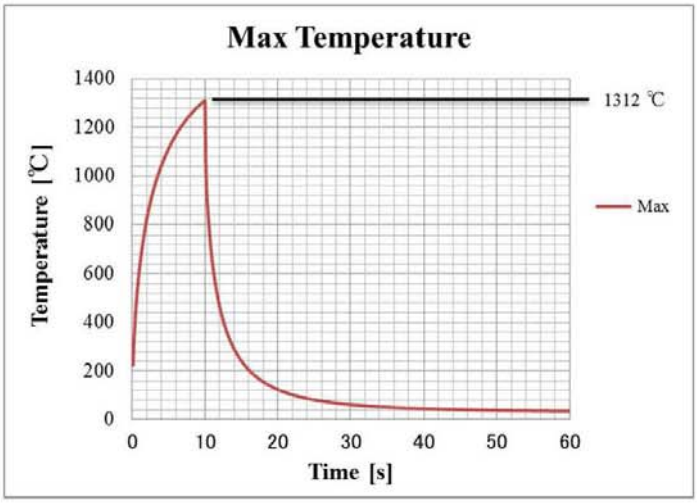

Fig. 5.1.6 Time dependence of the maximum temperature

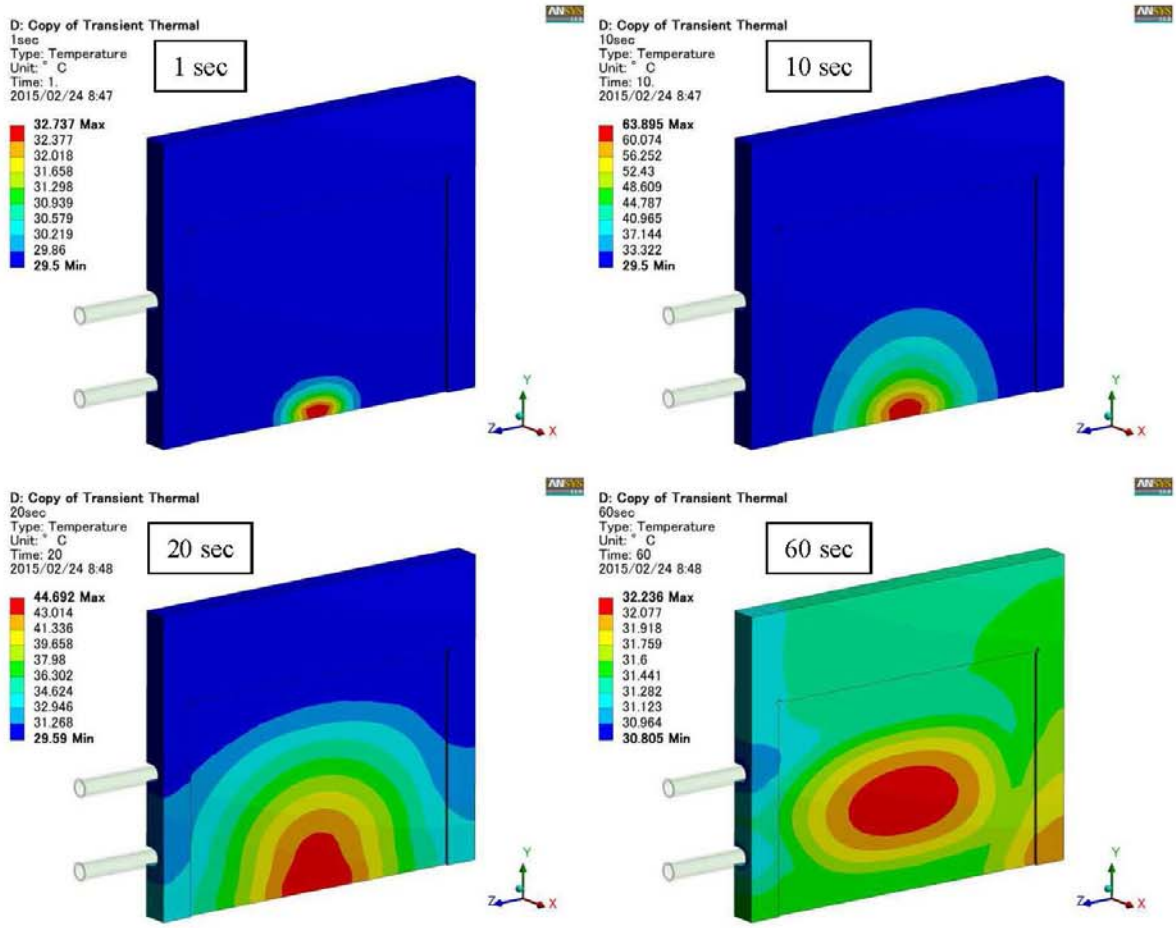

Fig. 5.1.7 Temperature profile (OFHC holder)

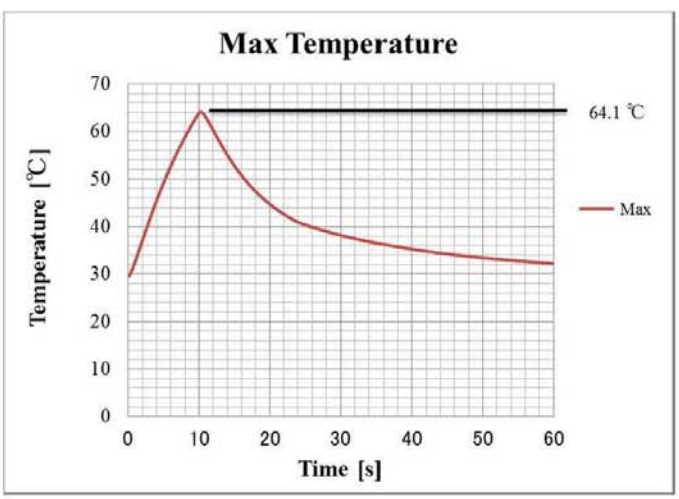

Fig. 5.1.8 Time dependence of the maximum temperature (OFHC holder)

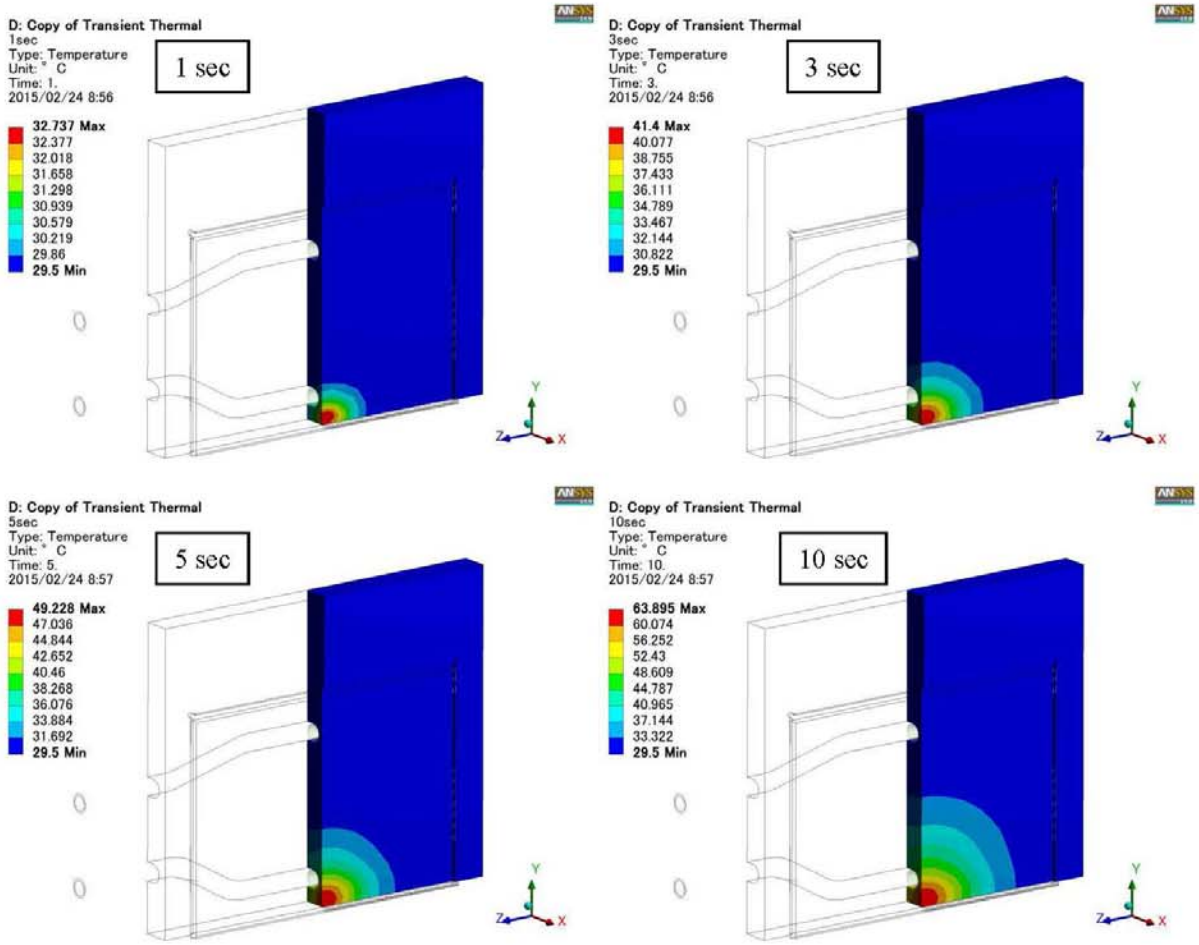

Fig. 5.1.9 Temperature profile (OFHC holder)

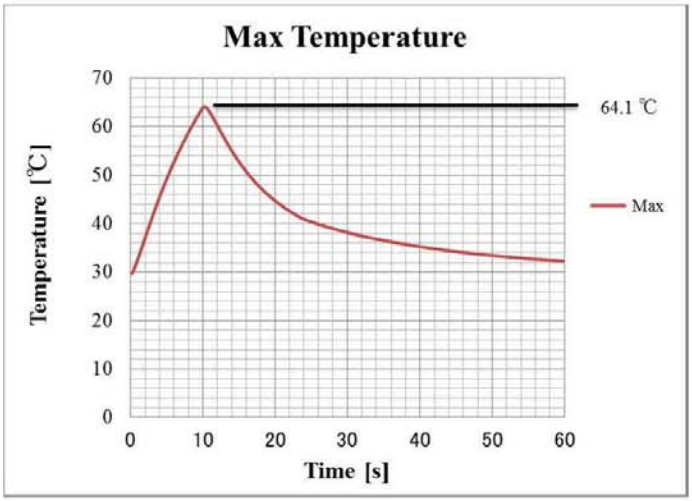

Fig. 5.1.10 Time dependence of the maximum temperature (OFHC holder)

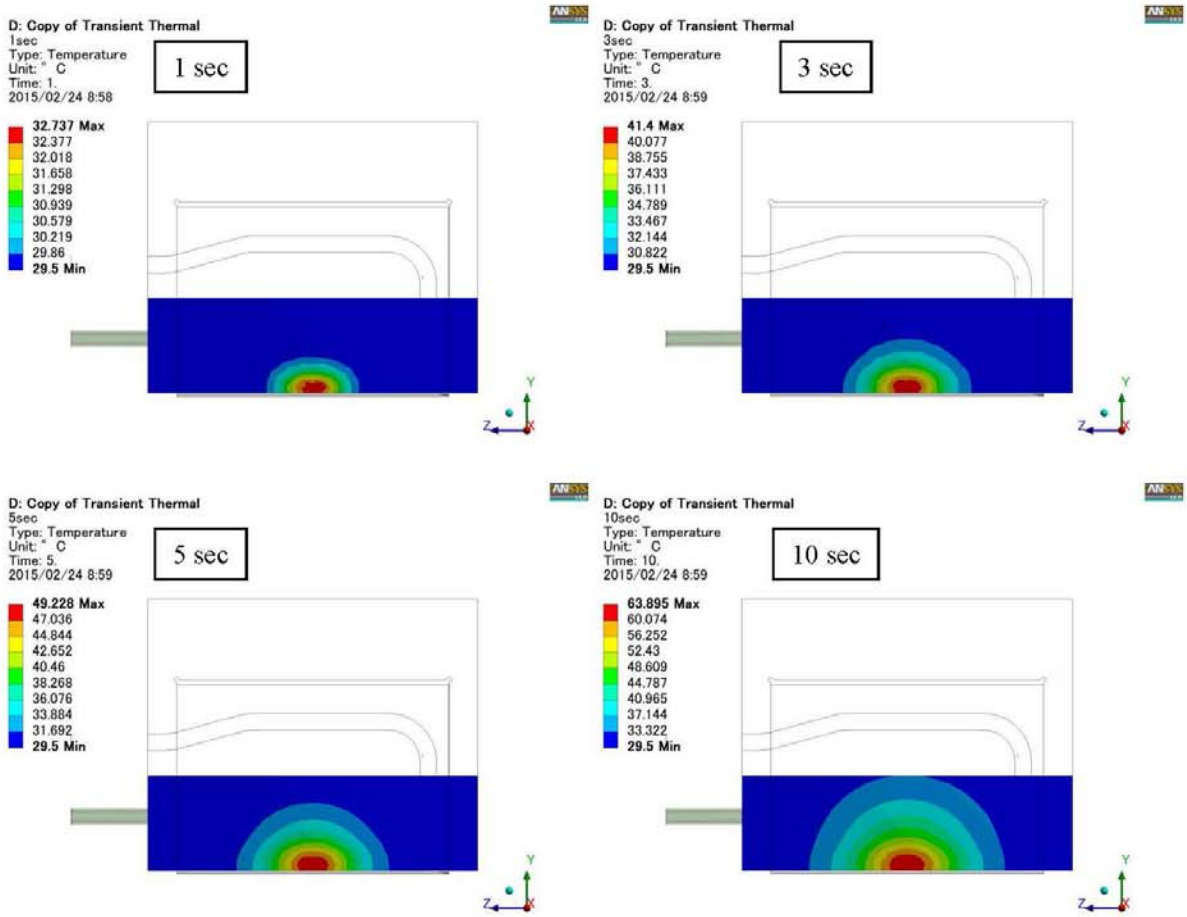

Fig. 5.1.11 Temperature profile (OFHC holder)

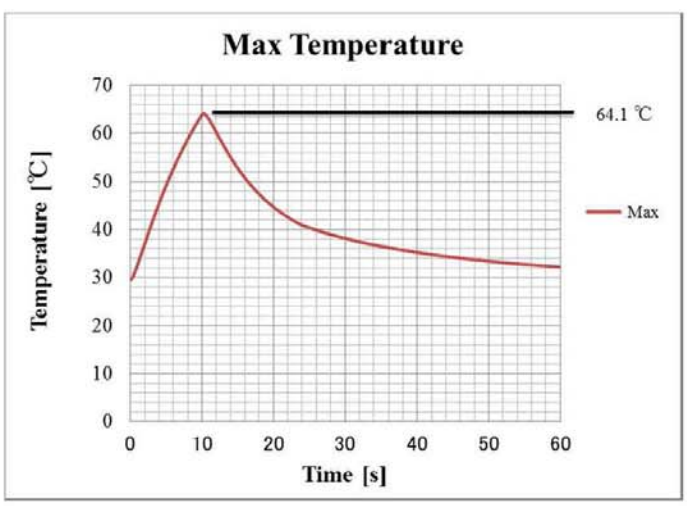

Fig. 5.1.12 Time dependence of the maximum temperature (OFHC holder)

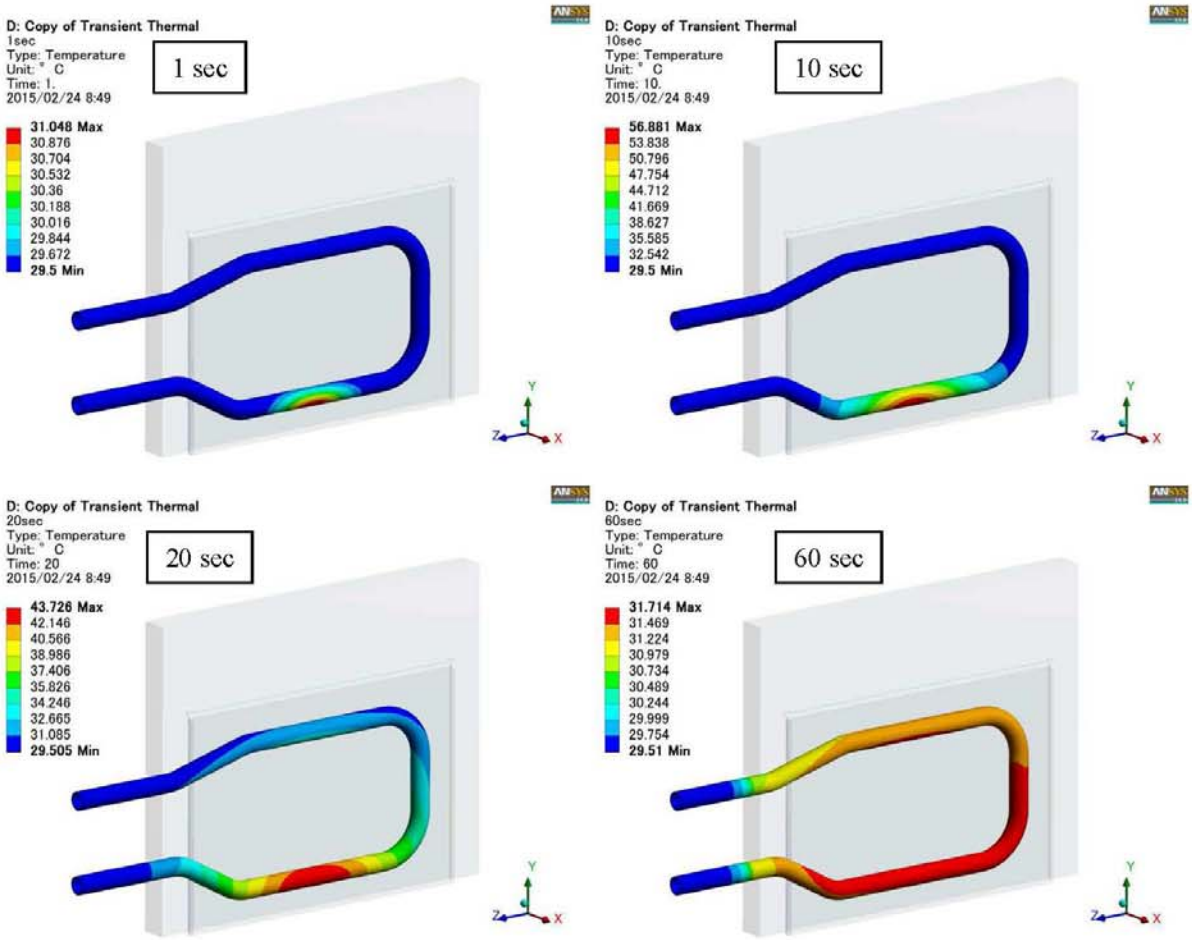

Fig. 5.1.13 Temperature profile (Cooling pipe)

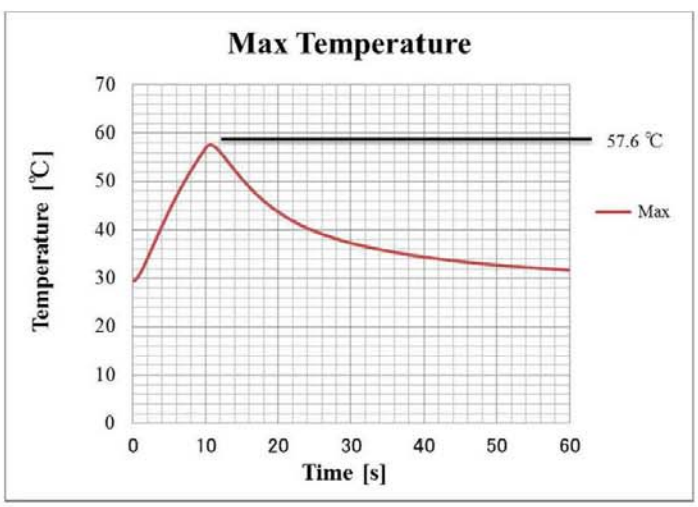

Fig. 5.1.14 Time dependence of the maximum temperature (Cooling pipe)